RSC Advances

PAPER

View Article Online
View Journal | View Issue

Cite this: *RSC Adv.*, 2022, **12**, 13367

Hybrid organic–inorganic membranes based on sulfonated poly (ether ether ketone) matrix and iron-encapsulated carbon nanotubes and their application in CO_2 separation

Aleksandra Rybak, *[a] Aurelia Rybak,[b] Sławomir Boncel,[a] Anna Kolanowska,[a] Waldemar Kaszuwara[c] and Spas D. Kolev[d]

Received 10th March 2022
Accepted 15th April 2022

DOI: 10.1039/d2ra01585d

rsc.li/rsc-advances

The need to reduce greenhouse gas emissions dictates the search for new methods and materials. Here, a novel type of inorganic–organic hybrid materials Fe@MWCNT-OH/SPEEK (with a new type of CNT characterized by increased iron content, 5.80 wt%) for CO_2 separation is presented. The introduction of nanofillers into a polymer matrix has significantly improved hybrid membrane gas transport (*D*, *P*, *S*, and α_{CO_2/N_2}), and magnetic, thermal, and mechanical parameters. It was found that magnetic casting has improved the alignment and dispersion of Fe@MWCNT-OH carbon nanotubes. At the same time, CNT and polymer chemical modification enhanced interphase compatibility and membrane CO_2 separation efficiency. The thermooxidative stability, and mechanical and magnetic parameters of composites were improved by increasing new CNT loading. Cherazi's model turned out to be suitable for describing the CO_2 transport through analyzed hybrid membranes. The comparison of the transport and separation properties of the tested membranes with the literature data indicates their potential application in the future and the direction of further research.

Introduction

Increasing industrialization and the development of civilization are associated with an increased demand for energy, which entails an excessive increase in the combustion of fossil fuels and CO_2 emissions.[1] The accumulation of CO_2, which accounts for more than half of greenhouse gas emissions, is responsible for global warming, rising sea levels, and severe climate change. Therefore, the current measures should aim to reduce emissions of greenhouse gases, in particular CO_2.[2] Various strategies for reducing CO_2 emissions are proposed, such as: reducing energy demand, implementing cleaner energy sources, reducing the carbon footprint, capturing, storing, or sequestering CO_2, and using CO_2 as a feedstock. Separated CO_2 can be used in enhanced oil recovery (EOR) operations, as well as in the cultivation of algae, phytoplankton, or bacteria, which allows the production of food, livestock feed, lipids, methane, biofuels, and even algal plastic called polyethylene furandicarboxylate (PEF).[3] Currently, technologies related to the capture and storage of CO_2 are the most promising. CO_2 storage strategies include geological, deep ocean storage, and fixation in inorganic carbonates.[4]

On the other hand, the CO_2 capture technology consists in its removal from technological streams or exhaust gases and its subsequent processing. There are three leading technologies to capture CO_2: pre-combustion, intra-combustion, and post-combustion.[5–17] The last of these technologies, consisting in the separation of CO_2 from flue gas, can be adapted to existing industrial plants, and the released CO_2 can be a substrate for subsequent processes. CO_2 separation can be performed using various conventional methods such as absorption, adsorption, chemical looping combustion, hydrate-based separation, and cryogenic distillation.[18–20] However, most of them are highly energy-consuming and costly. Therefore, the latest research is moving towards membrane methods, which require significantly lower financial outlays and energy consumption. Both polymeric and inorganic membranes are used in the separation of CO_2 from gas mixtures. However, both types have advantages and disadvantages.[18,19,21,22] Therefore, an excellent solution can be hybrid membranes, also known as mixed matrix membranes (MMMs). They combine the advantages of both a polymer matrix and inorganic additives. However, in such membranes, particular attention must be paid to the excellent dispersion of the inorganic phase and good compatibility of these two phases.[23–26] Usually, a combination of inorganic fillers (such as CNTs, graphene, silica, metal oxides, nanofibers, zeolites, MOF and POF,

[a]*Faculty of Chemistry, Silesian University of Technology, Strzody 7, 44-100 Gliwice, Poland. E-mail: aleksandra.rybak@polsl.pl*

[b]*Faculty of Mining, Safety Engineering and Industrial Automation, Silesian University of Technology, Gliwice, Poland*

[c]*Faculty of Materials Science and Engineering, Warsaw University of Technology, Warszawa, Poland*

[d]*School of Chemistry, The University of Melbourne, Victoria 3010, Australia*

CMS) with a polymer matrix (various types of polymers, such as polyimides (PI), fluorinated polyimides (FPI), polyamides, polysulfone (PSF), cellulose acetate (CA), polydimethylsiloxane (PDMS), poly(vinyl acetate) (PVAc), poly(2,6-dimethyl-1,4-phenylene oxide) (PPO), brominated sulfonated poly(2,6-dimethyl-1,4-phenylene oxide) (BSPPO), polyvinyl amine, *etc.*) leads to hybrid materials with improved gas transport, mechanical, thermal, electrical or magnetic properties.[27–36] Such materials can be achieved by controlling the filler additive's composition, content, and morphology, using various processing techniques, or by appropriate modification of both phases.[23,24,31,34] Thus, to increase the compatibility between the phases and reduce the particle size of the inorganic particles, multiwall nanotubes (MWCNTs) could be used as a new carbon filler. It is also possible to modify both the inorganic additive and the polymer matrix, forming bonds between the considered phases.

In recent years, the interest in CNTs has been due to their unique optical, magnetic, mechanical, thermal, and electrical properties. Due to their developed surface, many selective gas adsorption sites, and mechanical resistance, CNTs have also found application as fillers in hybrid membranes.[37–40] However, MWCNTs tend to aggregate in the polymer matrix, and therefore, to limit it and increase membrane permeability and selectivity, it is proposed to functionalize both the nanotubes and the polymer and introduce potential external fields.[40–43] Polymer matrices can be modified by acylation, carboxylation, bromination, and sulfonation.[44] The latter has been reported as a suitable method to increase the separation capacity of membranes.[45]

This paper reports the CO_2/N_2 separation results using new, magnetically aligned Fe@MWCNT-OH/SPEEK membranes with different additive contents. The higher content of iron characterized the applied Fe@MWCNTs. Aligning of Fe@MWCNTs in hybrid membranes at various magnetic-field inductions and chemical modification of the inorganic filler particles, polymer matrix, and their influence on CO_2 separation performance was investigated. The obtained membranes were also characterized by a static mechanical performance, transmission electron microscopy (TEM), scanning electron microscopy (SEM), thermogravimetry (TGA), X-ray diffraction (XRD), and vibrating sample magnetometry (VSM). The experimental results were compared with theoretically predicted data based on a three-phase system.

Experimental

Materials

Poly (ether ether ketone) (PEEK) was purchased from Evonik Industries AG (Germany). Sulfuric acid, *N*,*N*-dimethylacetamide (DMAc), toluene, ferrocene, methanol, iron(II) sulfate heptahydrate, trichloroethylene (TCE), and hydrogen peroxide of 99% purity were supplied by Chemiatrade (Poland). Carbon dioxide (5.5), nitrogen (5.0), and argon (5.0) compressed cylinders were purchased from Air Liquide (Poland).

Sulfonation of PEEK

PEEK was sulfonated according to the procedure described elsewhere.[46] It was first dried in an oven at 80 °C for 24 h before being sulfonated. Then, 14 g of PEEK was dissolved in 100 ml of sulfuric acid (H_2SO_4, 95–98%) for about three hours at room temperature and then vigorously stirred at 45 °C for the next eight hours. Subsequently, the polymer solution was precipitated in ice-cold deionized water by mechanical stirring. Finally, the precipitated polymer was filtered off, washed few times with deionized water until neutral pH, and then dried (24 h at room temperature and then at 60 °C in a vacuum oven for a further 24 h). The degree of sulfonation of SPEEK (60.04%) was determined by the titration method. The scheme of the PEEK sulfonation reaction is presented in Fig. 1.

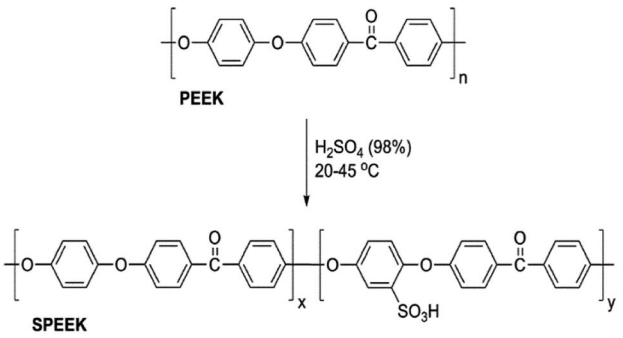

Fig. 1 Sulfonation of PEEK.

Synthesis and functionalization of Fe@MWCNTs

Fe@MWCNTs with increased iron content were self-synthesized by catalytic chemical vapor deposition (c-CVD) in an argon atmosphere (99.99%) at 760 °C, with a flow rate = 1.8 L min^{-1}, and the injection rate of the feedstock = 2.8 ml h^{-1}. A saturated solution of ferrocene (9.6 wt%; catalyst precursor) in toluene was used as the feedstock. In this case, Fe@MWCNTs saturated with iron were obtained in the form of thick layers of vertically oriented nanotubes with an outer diameter (OD) of 54 ± 31 nm and a length (*l*) of 100 ± 20 μm, a BET surface (a) of 34 m^2 g^{-1} and total iron content of 5.80 wt%.[38,47] The Fe@MWCNTs were then hydroxylated by adding iron(II) sulfate heptahydrate solution in deionized water (DIW) to which, after 15 minutes of ultrasonication, an aqueous solution of hydrogen peroxide (30 wt%) was added in one portion, and further sonicated for 12 hours. Thus, Fe@MWCNT-OH was separated on a PTFE membrane and washed with deionized water (DIW) and methanol. It was then dried at 80 °C for 72 h. It was found that their functionalization degree (df, mmol g^{-1}) was 3.5 mmol of OH group per 1 g of nanotube carrier.[48] On the other hand, the Fe : C ratio in the obtained Fe@MWCNT-OH remained unchanged, which indicates that the hydroxylation mechanism was based on the attack of hydroxyl radicals on the centers of crystallographic disturbances in the walls of graphene.

Hybrid membrane preparation and characterization

The homogeneous and inorganic–organic hybrid membranes based on a SPEEK matrix and various additions of Fe@MWCNT-OH as a filler (CNTs: 0.5–10.0 wt%) were examined. These membranes were made by casting filler particles sonicated

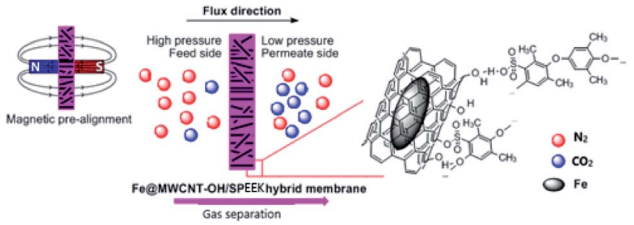

Fig. 2 Scheme of hybrid Fe@MWCNT-OH/SPEEK membrane preparation and gas permeation process.

dispersions in polymer solutions without or with the magnetic field (B = 40 mT or B = 100 mT) of two ferrite magnets at different distances (Fig. 2). The Fe@MWCNT-OH/SPEEK membranes were obtained from the dispersion of CNTs in a 9% SPEEK solution in DMAc, obtained by sonication for three hours. The suspensions thus prepared were poured into levelled Petri dishes and heated at 60 °C for 12 h, then at 80 °C for the next 12 h. By this procedure, a series of membranes with an inorganic content ranging from 0.5–10.0 wt% and thickness 100–200 μm were prepared. Gas (CO_2 and N_2) permeability measurements were carried out for membranes using the low-pressure gas permeation analyzer IDP-2, described elsewhere[49–51] at the temperature of 25 °C. These flow-rate data were used to obtain the mass transport coefficients (D, P, S, and α), using the Time Lag method.[52–55]

The mechanical and magnetic properties of obtained hybrid membranes were tested on a Zwick/Roell Z050 static testing machine and with the Lake Shore 7010 vibration magnetometer (VSM). On the other hand, the cross-sections of the membranes cut on the microtome were examined with the JEOL 1200 transmission electron microscope at an acceleration of 120 kV. It should be noted that a previous study of Fe@MWCNT alone using TEM showed that the iron is encapsulated in CNT.[47] TGA analysis was also performed at a heating rate of 10 °C min^{-1} under an argon atmosphere (60 ml min^{-1}) using a Linseis STA PT1600 thermobalance (Selb, Germany). Scanning electron micrographs of the obtained hybrid membranes were made with the SIX HITACHI S-3400N SEM apparatus. The samples were analyzed at 5 kV. The prepared membranes were also characterized using XRD (Rigaku Mini-Flex II diffractometer with Cu Kα radiation). The XRD and mechanical properties analysis was performed in the membrane thickness direction.

The evaluation of gas transport parameters through hybrid membranes

In order to analyze the mechanism of gas transport through the tested membranes, gas permeability tests for N_2 and CO_2 were carried out using a low-pressure gas permeation analyzer. For the analysis of experimental data, the Time Lag method was used, obtaining several significant gas transport coefficients, such as, $\bar{D}$, P, S, and α. During the gas permeation tests, the gas flow rate Q_{STP} was measured and then recalculated into diffusive mass flux J:

$$J = \frac{Q_{STP}}{A} \quad (1)$$

where Q_{STP} is a flow rate at standard conditions [cm_{STP}^3 s^{-1}], and A is a membrane-active area [cm^2].

Using J_S, permeation coefficient P was determined according to eqn (2):[52,53]

$$P = \frac{J_S\, l}{\Delta p} \quad (2)$$

where P is a permeation coefficient [barrer], [barrer = cm_{STP}^3 cm cm^{-2} s^{-1} cm_{Hg}^{-1} 10^{-10}], l is a membrane thickness [cm], Δp is a gas pressure difference at both sides of the membrane [cm_{Hg}], and J_S is a diffusive mass flux in a stationary state [cm_{STP}^3 cm^{-2} s^{-1}].

The following critical gas transport parameter was the average diffusion coefficient $\bar{D}$, obtained from the stationary state of permeation according to the equation:

$$\overline{D} = \frac{J_s \times l}{\Delta c_0} \quad (3)$$

where J_s is a diffusive mass flux in a stationary state [cm_{STP}^3 cm^{-2} s^{-1}], l is a thickness of the membrane [cm], and Δc_0 is the concentration difference [cm_{STP}^3 cm^{-3}].

After integration of mass flux J with respect to time was received a downstream absorption permeation $Q^a(l,t)$ (total flow of penetrant) from which the Δc_0 (intercept of the asymptote to the stationary permeation curve with the $Q^a(l,t)$ axis) could be determined using the Time Lag method.[52,53]

In turn, the solubility coefficient S is a measure of the size of sorption in membranes, and it was calculated from the eqn (4):

$$S = \frac{P}{\overline{D}} \quad (4)$$

where S is a solubility coefficient [cm_{STP}^3 cm^{-3} cm_{Hg}^{-1}].

The last parameter, the ideal selectivity coefficient α_{CO_2/N_2}, could be calculated from the ratio of the obtained permeation coefficients:

$$\alpha_{CO_2/N_2} = \frac{P_{CO_2}}{P_{N_2}} \quad (5)$$

where P_{CO_2}, P_{N_2} are permeation coefficients of pure carbon dioxide and nitrogen.

Modeling of Fe@MWCNT-OH/SPEEK

In order to reduce the number of experiments and investigate the effect of various parameters on membrane performance, many theoretical models were developed to predict gas permeation through hybrid membranes.

Most of the existing models are used to characterize the mixed matrix membranes with inorganic additives in the form of platelet and spherical particles. However, a relatively small number of models consider the influence of tubular particles on the gas transport process. The first is the Hamilton–Crosser (HC) model, which uses the analogy between thermal conduction and gas permeation in polymer composites.[56] The second is the Kang–Jones–Nair (KJN) model, based on the parallel-series resistance model.[57] However, both models can only be used to

predict gas transport through two-phase systems with ideal morphology. Interface defects, such as voids, characterize hybrid membranes. Therefore, such membranes should be considered three-phase systems, consisting of a polymer matrix, filler particles, and interfacial voids. One of the models based on this assumption is the model proposed by Chehrazi *et al.*[58] It uses the analogy between mass and heat transfer in polymer composites.

Two characteristic parameters were introduced to characterize the polymer-nanotube interface, such as interfacial thickness" (a_{int}) and "interfacial permeation resistance" (R_{int}). The effective gas permeation through an imperfect membrane can be described as follows:[58]

$$\frac{P_{eff}}{P_m} = \frac{3 + \varphi\left(\frac{2(d/a_{int}-1)}{d/a_{int}+1} + \frac{P_{NT}/P_m}{1+\frac{2a_{int}}{L}\frac{P_{NT}}{P_m}} + \frac{L}{a_{int}} - 1\right)}{3 - \varphi\frac{2(d/a_{int}-1)}{d/a_{int}+1}} \quad (6)$$

where, P_{eff}, – the gas permeation coefficient of the MMM, P_m – the gas permeation coefficient of the polymer matrix, P_{NT} – the gas permeation coefficient of nanotube, φ – volume fraction of nanotubes, a_{int} – thickness of the interfacial region that connects chemically or mechanically the nanotubes and the polymer matrix phases and plays a crucial role in the entire properties of composites, L – length of the nanotube, d – diameter of the nanotube.

In order to compare the predicted results with experimental data from our own research, the average absolute relative error (AARE) was calculated as follows:[50,59]

$$\%\ \text{AARE} = \frac{100}{\text{NDP}}\sum_{i=1}^{\text{NDP}}\left|\frac{P_i^{pred} - P_i^{exp}}{P_i^{exp}}\right| \quad (7)$$

where, NDP – the number of data points, P_i^{pred} – the predicted permeability value, P_i^{exp} – the experimental permeability value.

This article compares the obtained experimental results with the results predicted using the theoretical model developed by Chehrazi *et al.*[58] Therefore, the values of P_{eff}/P_m for CO_2 were calculated, using the relationship given in eqn (6), assuming that L = 10 000 nm, d = 10 nm, and changing one of the parameters, respectively, while the others remain constant. The values of P_{NT}/P_m, φ, and a_{int} were varied in the following ranges 1–10 000, 0.005–0.1, and 50–500 nm, respectively. The values of the changed parameters were selected so that the average absolute relative error %AARE was as small as possible. The comparison of the simulation and experimental results are presented in Table 3.

Results and discussion

Magnetic parameters of hybrid membranes

The magnetic parameters of hybrid membranes were investigated due to the significant influence of the magnetic field on the formation process of these membranes and their subsequent properties. Hysteresis loops were used to determine the saturation and coercivity magnetization, as shown in Fig. 3a. In turn, the next figures show the effect of Fe@MWCNT-OH content on the magnetic properties of the obtained membranes (Fig. 3b and c).

The shape of the hysteresis loop and the saturation magnetization show the paramagnetic nature of the SPEEK membrane and the slightly ferromagnetic nature of the membranes with the addition of modified Fe@MWCNT-OH (Fig. 3a).

In hybrid membranes based on the SPEEK matrix, a certain order of nanotubes has already been found, despite the lack of a magnetic field during their casting, which could be associated with interactions between the inorganic and polymer phases. Of

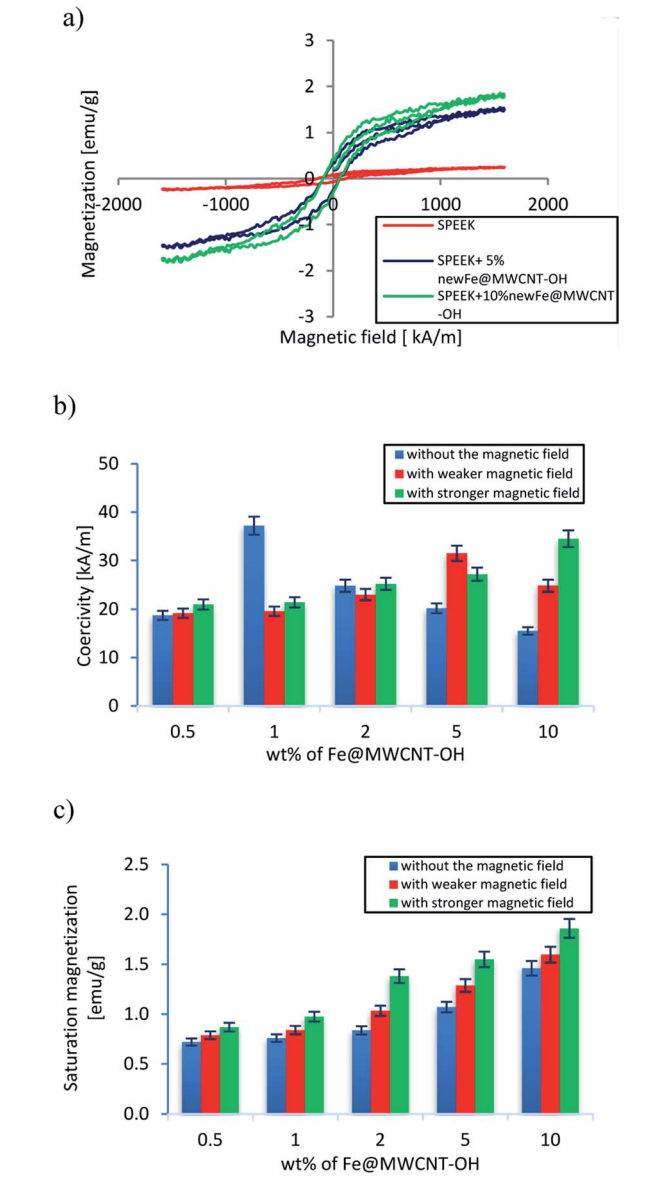

Fig. 3 Magnetic properties of hybrid membranes: (a) hysteresis loops of SPEEK, and Fe@MWCNT-OH/SPEEK membranes with 5 and 10 wt% of Fe@MWCNT-OH, (b) dependence of coercivity and (c) dependence of saturation magnetization of hybrid membranes cast in the absence and in the presence of weaker and stronger magnetic field on Fe@MWCNT-OH loading.

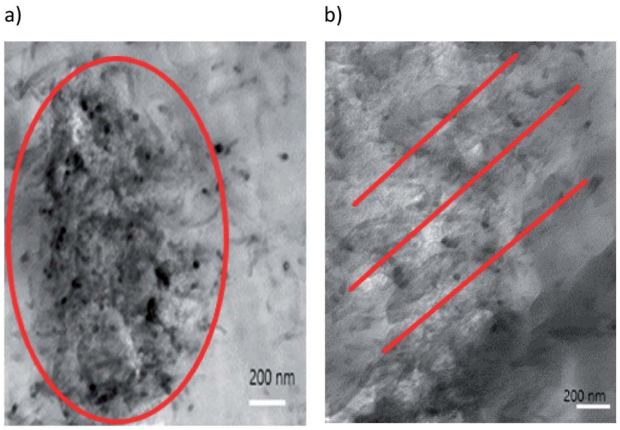

Fig. 4 Transmission electron microscopy (TEM) image of cross-sections of (a) Fe@MWCNT-OH/SPEEK membranes cast in a weaker magnetic field (area occupied by CNT aggregates is marked in red) and (b) Fe@MWCNT-OH/SPEEK membranes cast in a stronger magnetic field (10 wt% of Fe@MWCNT-OH) (the orientation of CNTs after applying the magnetic field is marked in red).

course, along with the increase in the strength of the magnetic field, better and better ordering was observed, which was reflected in the increase in both the coercivity and saturation magnetization values (Fig. 3b and c).

Membranes cast without the presence of a field or in a lower magnetic field were characterized by some coercive disorders, especially with a higher addition of CNTs, which may be related to the formation of aggregates (shown in Fig. 4a). However, this phenomenon was not observed in the stronger magnetic field, where the coercivity value increased with the increase of the inorganic addition. This may be related to better CNT-OH dispersion in the modified matrix and their better arrangement in the structure of the hybrid membrane (Fe@MWCNT-OH are aligned according to the magnetic-field lines – Fig. 4b).

Comparing the magnetic properties of membranes based on the new carbon nanotubes with a higher Fe content (5.80 wt%) with membranes based on the previous type of CNTs with a lower Fe content, a slight increase in the coercivity and magnetization values was found. But this slight increase certainly contributed to the improvement of the dispersion of nanotubes in the polymer matrix and had a positive effect on the separation and mechanical properties of the membranes. This may be related to the faster and more effective response of CNTs to the influence of an external magnetic field.

The above conclusions regarding the morphology of hybrid membranes were also confirmed by SEM analysis. Hybrid membranes based on the SPEEK matrix cast without the influence of the magnetic field were characterized by the presence of CNTs aggregates (Fig. 5a). After introducing an external magnetic field during the production of membranes, a much better dispersion of inorganic particles in the polymer matrix was achieved (Fig. 5b). The TEM image shows a specific arrangement of nanotubes along the magnetic field lines in the form of visible bands. On the other hand, the best morphological properties were demonstrated by hybrid membranes

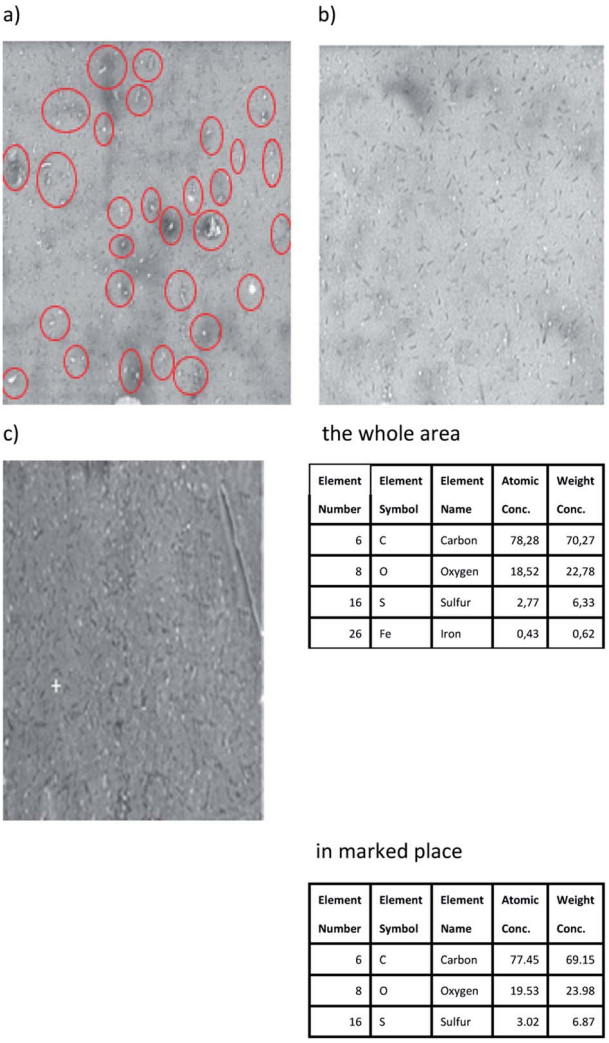

Element Number	Element Symbol	Element Name	Atomic Conc.	Weight Conc.
6	C	Carbon	78,28	70,27
8	O	Oxygen	18,52	22,78
16	S	Sulfur	2,77	6,33
26	Fe	Iron	0,43	0,62

Element Number	Element Symbol	Element Name	Atomic Conc.	Weight Conc.
6	C	Carbon	77.45	69.15
8	O	Oxygen	19.53	23.98
16	S	Sulfur	3.02	6.87

Fig. 5 SEM images of: (a) Fe@MWCNT-OH/SPEEK membranes (1 wt%) cast without a magnetic field (areas occupied by CNT aggregates are marked in red), (b) Fe@MWCNT-OH/SPEEK membranes (1 wt%) cast in a stronger magnetic field, (c) Fe@MWCNT-OH/SPEEK (5 wt%) membranes cast in a stronger magnetic field.

based on a modified polymer matrix and Fe@MWCNT-OH nanotubes cast in a stronger magnetic field, where a combined effect of both the introduced functionalizations and the influence of the magnetic field on the improvement of nanotube dispersion and the increase in compatibility between the analyzed phases was observed (Fig. 5c).

Mechanical properties of obtained hybrid membranes

Bearing in mind the future potential application of the tested membranes, their mechanical properties should also be examined. Therefore, two mechanical parameters were investigated, such as Young's modulus (E) and tensile strength (R_m) (Fig. 6).

In the case of hybrid membranes cast without the influence of an external magnetic field, an increase in tensile strength R_m was noted until filler loading was 2 wt% (from 36.32 to 43.69 MPa). However, for higher additives, a decrease in the value of this parameter was found (22.90 MPa). While the value of

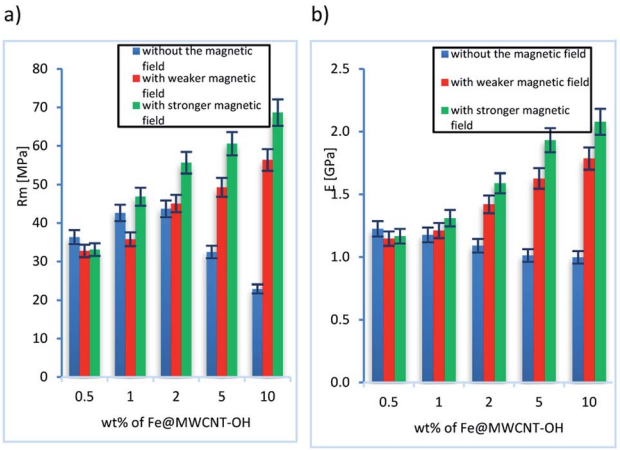

Fig. 6 Mechanical properties of hybrid membranes: (a) R_m *vs.* Fe@MWCNT-OH loadings for SPEEK membranes cast in the absence and in the presence of weaker and stronger magnetic field and (b) *E versus* Fe@MWCNT-OH loadings for SPEEK membranes cast in the absence and in the presence of weaker and stronger magnetic field.

Young's modulus *E* for these membranes decreased slightly with the increase of CNTs addition (from 1.23 to 1.00 GPa). On the other hand, the introduction of a weak magnetic field in the membrane production process allowed to increase both the tensile strength R_m (from 32.73 to 56.32 MPa) and the Young's modulus *E* (from 1.15 to 1.78 GPa). The increase in Young's modulus *E* may be due to an increase in the density of ionic physical crosslinking between polar ionic sites. Obviously, thanks to the mutual influence of both the applied chemical modifications, leading to the formation of bonds, and the influence of the external magnetic field, influencing the proper placement of nanotubes in the membrane structure, it allowed to obtain the highest values of mechanical parameters, even with the greatest inorganic addition (R_m from 33.09 to 68.64 MPa and *E* from 1.17 to 2.08 GPa), exceeding values for dense polymer membranes. The improvement of the mechanical properties of hybrid membranes may be related to the increase of density and reduction of the mobility of polymer chains, appropriate dispersion, and arrangement of nanotubes in the structure of hybrid membranes. Of course, this will directly translate into better separation properties of the membranes and their possible future use.

Fig. 7 shows the XRD spectra for a pure SPEEK membrane and a hybrid membrane with the addition of 2 wt% Fe@MWCNT-OH. XRD analysis revealed the SPEEK semi-crystalline structure (peak at 21.5°). Comparing the obtained spectra with the literature data for PEEK,[60,61] it should be noted that the polymer changed to a partially amorphous form after carrying out sulfonation. On the other hand, after the addition of modified nanotubes Fe@MWCNT-OH, the appearance of peaks corresponding to several Fe-phases (42.9° for α-Fe and 44.7° for γ-Fe) and graphite shells (25.8° and 42.3°) was found. Their presence was confirmed during an earlier XRD analysis of pure Fe@MWCNT.[61] Overlapping between the peaks, characteristic for the polymer matrix and the inorganic additive was

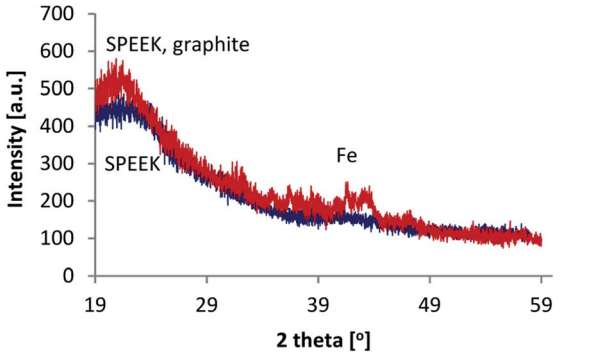

Fig. 7 X-ray diffraction spectra for SPEEK and Fe@MWCNT-OH/SPEEK membrane (2 wt%).

stated. A certain increase in the peak intensity after the introduction of the modified nanotubes can be associated with an appropriate incorporation of Fe@MWCNT-OH into the SPEEK polymer matrix.

Thermal analysis of SPEEK/Fe@MWCNT-OH membranes

TGA was carried out to study the thermal stability of membranes as shown in Fig. 8.

It was indicated that all membranes showed similar few steps of the weight loss. While for the Fe@MWCNT-OH/SPEEK composites the following stages of weight loss have been noted. The first one, below 190 °C corresponds with loss of water and residual solvent in membranes. The second weight loss from 211–360 °C was caused by the degradation of sulfonic groups from SPEEK matrix and degradation of OH groups from Fe@MWCNT-OH. The last weight loss from 517–800 °C is related with the degradation of main polymer chain and oxidation of Fe@MWCNT-OH.

It should be noted that with the increase of Fe@MWCNT-OH addition, the maximum of the peaks responsible for the subsequent transformations are shifted towards higher temperatures. This may indicate better thermo-oxidative properties of the obtained hybrids, despite the use of the SPEEK

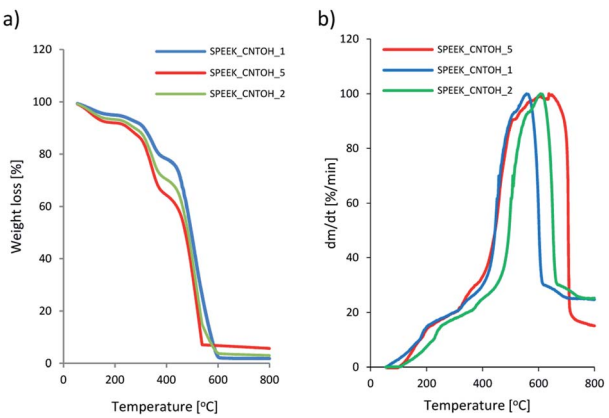

Fig. 8 TGA and DTG results for Fe@MWCNT-OH/SPEEK hybrid membranes with various Fe@MWCNT-OH addition.

Table 1 CO_2 and N_2 gas transport parameters of (a) Fe@MWCNT-OH/SPEEK membranes prepared in the absence and (b) in the presence of the stronger magnetic field

Membrane Fe@MWCNT-OH/SPEEK with Fe@MWCNT-OH (wt%)	α_{CO_2/N_2}	N_2			CO_2		
		$\bar{D}$ 10^8 (cm^2 s^{-1})	P (barrer)	S 10^2 (cm_{STP}^3 cm^{-3} cm_{Hg}^{-1})	$\bar{D}$ 10^8 (cm^2 s^{-1})	P (barrer)	S 10^2 (cm_{STP}^3 cm^{-3} cm_{Hg}^{-1})
(a)							
0.0	34.00	2.00 ± 0.18	0.45 ± 0.04	0.23 ± 0.02	4.80 ± 0.33	15.30 ± 1.07	3.19 ± 0.22
0.5	35.98	2.30 ± 0.20	0.50 ± 0.04	0.22 ± 0.02	5.04 ± 0.35	18.05 ± 1.26	3.58 ± 0.25
1.0	36.93	2.37 ± 0.22	0.52 ± 0.05	0.23 ± 0.02	5.09 ± 0.36	19.28 ± 1.35	3.79 ± 0.26
2.0	40.07	2.74 ± 0.25	0.63 ± 0.06	0.23 ± 0.02	5.14 ± 0.37	25.25 ± 1.77	4.92 ± 0.34
5.0	41.37	3.20 ± 0.29	0.81 ± 0.07	0.25 ± 0.02	5.18 ± 0.36	33.51 ± 2.34	6.46 ± 0.45
10.0	40.98	3.30 ± 0.30	0.86 ± 0.08	0.26 ± 0.03	5.49 ± 0.38	35.04 ± 2.45	6.38 ± 0.45
(b)							
0.0	34.00	2.00 ± 0.18	0.45 ± 0.04	0.23 ± 0.02	4.80 ± 0.33	15.30 ± 1.07	3.19 ± 0.22
0.5	36.34	3.25 ± 0.29	0.60 ± 0.05	0.18 ± 0.01	5.44 ± 0.38	21.66 ± 1.51	3.98 ± 0.28
1.0	40.41	3.36 ± 0.29	0.62 ± 0.05	0.19 ± 0.02	5.57 ± 0.39	25.06 ± 1.75	4.52 ± 0.32
2.0	47.22	3.88 ± 0.35	0.75 ± 0.07	0.19 ± 0.02	5.69 ± 0.39	35.34 ± 2.47	6.25 ± 0.43
5.0	52.23	4.53 ± 0.40	0.96 ± 0.08	0.21 ± 0.02	5.78 ± 0.40	50.26 ± 3.51	8.71 ± 0.60
10.0	58.63	4.67 ± 0.42	1.02 ± 0.09	0.22 ± 0.02	5.89 ± 0.41	59.56 ± 4.17	10.12 ± 0.71

matrix. The temperature corresponding to the 5 wt% weight losses during thermooxidative degradation increased with increasing content of CNTs in the materials (*e.g.*, from 198 °C for hybrid Fe@MWCNT-OH/SPEEK with 1 wt%, 211 °C for hybrid SPEEK with 2 wt%, to 225 °C for hybrid SPEEK with 5 wt% of CNT-OH). So, we can see, that TGA results confirmed the thermooxidative stability of the analyzed membranes. The thermo-oxidative properties of the obtained composite membranes proved their potential use in CO_2 separation. The weight loss of the hybrid membranes was lower than that of the pure membrane and decreased with increasing Fe@MWCNT-OH content. It should be noted that hybrid membranes would not degrade below 225 °C, indicating that they can potentially be used in CO_2 separation.

Gas transport characteristics of Fe@MWCNT-OH/SPEEK hybrid membranes

When designing membranes with a potential subsequent application for the separation of CO_2 from gas mixtures, possible problems related to plasticization and swelling of the membranes should be taken into account. This can result in an increase in spacing between the polymer chains and a reduction in the selectivity of the separation process. Therefore, the development of CO_2 selective membranes focuses on the synthesis of polymers with shape-stable and high chain stiffness. Membranes with a degree of sulfonation of 40% do not show the phenomenon of plasticization up to 11 bar, while with a degree of over 40% up to 32 bar.[44] In the above paper, modification of the polymer matrix by sulfonation was applied. Thanks to this process, membranes with a high degree of sulfonation were obtained, which protects them against possible plasticization by tightening the polymer chains.

The synthesized hybrid membranes were examined for their potential use in CO_2 separation. Table 1 shows the parameters of CO_2 and N_2 transport through the tested Fe@MWCNT-OH/SPEEK membranes. The results were obtained based on six-fold measurements of three identical hybrid membranes. The reproducibility of the method was checked by the Hartley F_{max} test. It was found that the obtained values of the standard deviation did not differ in a statistically significant manner ($F_{max} < F_{max\ o}$ (2.9 < 11.1)). Therefore, it was possible to calculate the mean value and the reproducibility value of the procedure was CV = 8.74% for each measurement series.

Comparison of experimental and theoretically predicted data (using the Chehrazi model) for the synthesized hybrid Fe@MWCNT-OH/SPEEK membranes (cast in a different magnetic field) is presented in Table 2. It can be seen that the thickness of the interphase a_{int} between the organic and inorganic phases decreases several times with increasing magnetic field induction (for hybrid membranes without a magnetic field: $a_{int} = 200$, with a magnetic field $B = 40$ mT : $a_{int} = 150$ and with a magnetic field $B = 100$ mT : $a_{int} = 100$). Such a measurable reduction in interphase thickness may be associated with better compatibility and interfacial interaction. It was also found that the observed phenomenon has a positive effect on the transport properties of the tested hybrid membranes.

On the other hand, taking into account the value of the ratio of the CO_2 permeability coefficient through nanotubes to the permeability through the polymer matrix P_{NT}/P_m, it was found that it increases with increasing magnetic field induction (for hybrid membranes cast without a magnetic field: $P_{NT}/P_m = 100$, in field $B = 40$ mT : $P_{NT}/P_m = 5000$ and in the field $B = 100$ mT : $P_{NT}/P_m = 10\,000$). This may indicate not only better compatibility between the modified organic and inorganic phases, reduction of possible defects, but also a positive influence of the magnetic field on the gas transport properties of the obtained membranes. The % AARE error ranged from 12–16%, which may indicate the appropriateness of the Chehrazi model

Table 2 Experimental and theoretically predicted data for the Fe@MWCNT-OH/SPEEK hybrid membranes, cast under various conditions

Membrane	φ	Experimental data $P_{eff}/P_{m_{CO_2}}$	Theoretical data $P_{eff}/P_{m_{CO_2}}$	Parameters for simulation	AARE [%]
SPEEK/Fe@MWCNT-OH without magnetic field	0.005	1.18	1.11		12.40
	0.010	1.26	1.22	$a_{int} = 200$	
	0.020	1.65	1.43		
	0.050	2.19	2.06	$P_{NT}/P_m = 100$	
	0.100	2.29	3.06		
SPEEK/Fe@MWCNT-OH in weak magnetic field	0.005	1.36	1.16		14.60
	0.010	1.45	1.32	$a_{int} = 150$	
	0.020	1.90	1.63		
	0.050	2.52	2.54	$P_{NT}/P_m = 5000$	
	0.100	2.98	4.00		
SPEEK/Fe@MWCNT-OH in strong magnetic field	0.005	1.42	1.24		16.60
	0.010	1.64	1.48	$a_{int} = 100$	
	0.020	2.31	1.96		
	0.050	3.29	3.36	$P_{NT}/P_m = 10\,000$	
	0.100	3.89	5.60		

for the description of CO_2 transport through the analyzed membranes. Such a correlation may prove that the influence of possible defects of the membrane structure on the gas permeability in an imperfect three-phase system was considered.

However, comparing the theoretical and experimental data for successive increasing CNT-OH additives, it can be concluded that up to 5 wt% the consistency of the results is high. On the other hand, the greatest deviation between the results was found for the largest addition of 10 wt%, which indicates the need for further modification of the proposed model in the future.

When analyzing the obtained results, one should take into account the influence of the modified SPEEK polymer matrix and carbon nanotubes, as well as their mutual influence on the transport of the tested gases through the Fe@MWCNT-OH/SPEEK hybrid membranes. In previous studies[49–55] on hybrid membranes, it was found that casting of the membranes in an external magnetic field improved the transport properties of gases to some extent. However, only the modification of both the polymer matrix and the inorganic additive allowed for the creation of hydrogen bonds and significantly improved the compatibility of both phases and the transport properties of oxygen. Therefore, in the above work, the authors immediately decided to functionalize Fe@MWCNT by hydroxylation and the poly (ether ether ketone) matrix by sulfonation. This enabled the enhancement of the interaction between both phases by creating hydrogen and sulfonate bonds (between $-SO_3H$ groups from the polymer matrix and –OH from CNTs), which in turn measurably reduced the defects at the interface and improved the transport and mechanical properties of the produced membranes. The combination of the positive influence of a stronger external magnetic field and the modification of membrane's both components made it possible to obtain membranes not burdened with the negative influence of forming clusters and interfacial defects. The introduction of the magnetic field contributed to the proper ordering of the internal structure of membranes, especially CNT in the polymer matrix, and the creation of ordered transport pathways for CO_2. Thus, we see that magnetic casting may prove to be a suitable method to improve the performance of hybrid membranes used in the separation of CO_2 from gas mixtures. Therefore, there was an increase in the value of CO_2 transport coefficients with the increasing addition of nanotubes, without any drops for

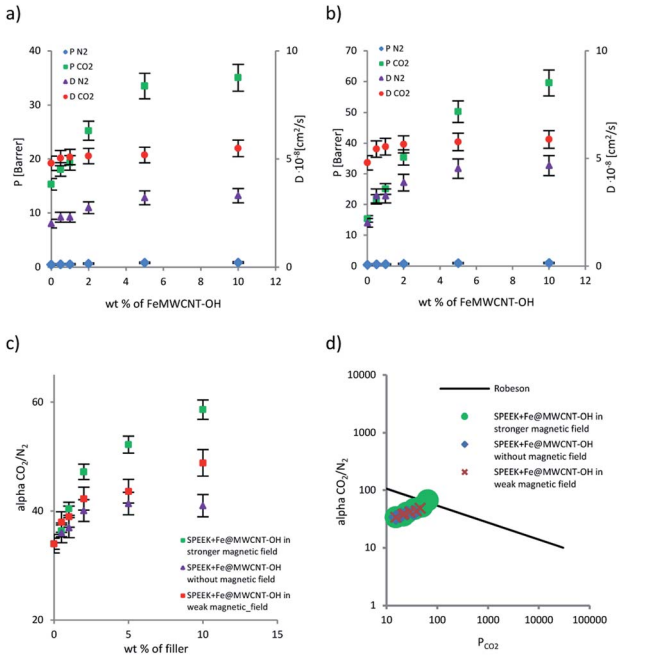

Fig. 9 Dependence of the gas transport coefficients: (a) permeation and diffusion coefficients *versus* Fe@MWCNT-OH loading in the SPEEK hybrid membranes cast in the absence of magnetic field, (b) cast in the stronger magnetic field, (c) selectivity coefficient α_{CO_2/N_2} *versus* filler concentration in the various hybrid membranes and (d) selectivity coefficient α_{CO_2/N_2} *versus* permeation coefficient P_{CO_2} regarding the Robeson upper bound line.

higher additives, as was the case with unmodified membranes. Obviously, sulfonation of the polymer matrix resulted in an increase in the selectivity coefficients α_{CO_2/N_2} (from 20.00 to 34.00) and a decrease in the permeability coefficients of CO_2 (P_{CO_2} from 37.50 to 22.49) and N_2 (P_{N_2}: from 1.20 to 0.78).[62] This is most likely due to an increase in density and a decrease in the mobility of the polymer chains as a result of stronger interchain interactions. The applied modifications and the use of the magnetic field made it possible to obtain hybrid membranes characterized by an increase in the coefficients of permeability, diffusion, sorption and even selectivity α_{CO_2/N_2} (from 34.00 to 58.63) with the Fe@MWCNT-OH loading rise (Table 1 and Fig. 9).

For the permeability coefficient P_{CO_2}, a significant increase was noted with the increase in the nanotube content, in particular after the use of a stronger magnetic field (P_{CO_2} from 15.30 to 35.04 without magnetic field and from 15.30 to 59.56 with stronger magnetic field). This increase may be related to the increase in the stiffness of the polymer chains, the greater FFV and the mobility of CO_2 molecules. At the same time, with the increase of inorganic addition, the values of the diffusion D_{CO_2} and sorption S_{CO_2} coefficient increased (D_{CO_2}: from 4.80 to 5.49 $\times$ 10^{-8} and S_{CO_2}: from 3.19 to 6.38 $\times$ 10^{-2} without magnetic field and D_{CO_2}: from 4.80 to 5.89 $\times$ 10^{-8} and S_{CO_2}: from 3.19 to 10.12 $\times$ 10^{-2} with stronger magnetic field). Thus, we can see that the increase in the CO_2 permeability coefficient may be the result of an increase in the value of both these coefficients, but in particular the sorption coefficient (due to lower crystallinity, increase of fractional free volume and the interaction of CO_2 with both modified polymer matrix and Fe@MWCNT-OH).

On the other hand, the nitrogen permeability coefficient P_{N_2} also showed a slight increase (from 0.45 to 0.86 without magnetic field and from 0.45 to 1.02 with stronger magnetic field), which may be caused by a small rise of the diffusion coefficient value D_{N_2} in the changed structure of the hybrid membrane (from 2.00 to 3.30 $\times$ 10^{-8} without magnetic field and from 2.00 to 4.67 $\times$ 10^{-8} with stronger magnetic field). On the other hand, the values of the sorption coefficient S_{N_2} did not change or even slightly decreased with the increasing addition of CNT in a stronger magnetic field.

It should be noted that the presence of sulfonic and sulfonate groups provides strong molecular interactions with CO_2 and favorable affinity for CO_2. Higher degree of sulfonation gives higher efficiency of gas separation because sulfonic groups can form hydrogen bonds and strong molecular interactions with CO_2. The high polarity of the sulfonic groups may promote CO_2–sulfone interactions, allowing a favorable affinity for CO_2. Also, the greater compatibility of the sulfonated polymer matrix with the modified CNTs alleviates the interface defects and regulates the effective FFV to increase CO_2 diffusion. The introduction of polar sulfonic groups into the polymer matrix resulted in more compact packing of the polymer chains, which in turn allowed to obtain greater selectivity with much better efficiency than in the case of PEEK membranes. The sulfonic groups create specific uninterrupted CO_2 transport pathways, which leads to an increase in CO_2 solubility selectivity of the tested membranes. The introduction of an inorganic additive made it possible to create more tortuous pathways for N_2 as a larger molecule, resulting in an increase in selectivity. Thus, we see that sulfonation on the one hand improves interphase compatibility and reduces interfacial defects. On the other hand, the introduction of modified CNT-OH enhances the chain rigidity of the polymer and broadens the CO_2-philic pathways near the polymer-filler interface, which increased the selectivity. It was noticed that the permeability and selectivity increased with increasing additive content.

In turn, due to the fact that carbon dioxide is the main point of interest, its characteristic parameters should be taken into account, which play an important role in the process of gas transport through hybrid membranes and separation. It is important that the carbon dioxide molecule, due to its symmetry, has a constant electric quadrupole moment. Such quadrupoles can interact with the three-dimensional structure of the ordered "supra-structures" formed by Fe@MWCNTs in the polymer matrix of hybrid membranes. And this, in turn, causes the penetration of CO_2 into the cavities created there. On the other hand, a nitrogen molecule with a much smaller quadrupole moment will not interact with this three-dimensional structure. Thus, the effectiveness of adsorption and separation of gases such as CO_2/N_2 will be influenced by the nature of the 3D structure as well as the presence of oxygen (hydroxyl) groups in Fe@MWCNT-OH. In addition, the use of MWCNTs as a filler with a highly developed structure allowed for a significant improvement in the adsorption properties, which may be due to the increase in the energy of interaction of CO_2 molecules with "supra-structures" created by Fe@MWCNT-OH in the polymer matrix. This is reflected in the increasing CO_2 permeability and selectivity of the tested hybrid membranes with the increasing inorganic additive (Fig. 9b and c). An important element is also the approach of the measurement points to the Robeson's upper bound line (Fig. 9d) with the increase of filler addition, and even crossing this line by the membrane with the highest 10 wt% addition of Fe@MWCNT-OH. The crossing of the Robeson's line indicates the possibility of the potential use of the proposed membranes for industrial applications, as this line was determined on the basis of the latest experimental data on the separation of the CO_2/N_2 mixture. Summing up, it should be stated that reducing the size of the filler particles, introducing Fe atoms, but most of all hydroxylation of the CNT surface and sulfonation of the polymer matrix significantly increase the efficiency of CO_2/N_2 separation. This is most likely due to the electrical nature of the CO_2 molecule, which has a quadrupole moment and therefore interacts much more strongly with the polar groups than does the nitrogen molecule. It can therefore be concluded that more efficient membranes were obtained by modifying both the inorganic additive and the organic polymer matrix, as well as by casting the membranes in an external magnetic field.

Table 3 presents literature data on CO_2 separation with the use of hybrid membranes based on various polymer matrices and CNTs. On the other hand, Fig. 10 compares the results of CO_2 separation for the proposed Fe@MWCNT-OH/SPEEK hybrid membranes with the corresponding literature results, collected in Table 3.

Table 3 Gas transport properties of hybrid membranes based on various types of CNTs and polymer matrices

Hybrid membrane polymer matrix	Filler of hybrid membrane	CNT [wt%]	Pressure [bar]	Temperature [°C]	P_{CO_2} [barrer]	Alpha CO_2/N_2	Ref.
Cellulose acetate	CNT	0.1	3	—	147	5.50	63
BrPPO	CNT	5	0.67	25	153	28.00	64
Polyimide	CNT	15	1	25	866.6	4.10	65
CMC	CNT	1	2	80	116	45.00	66
PC/PEG	C-MWCNT	10	2	25	20.32	52.1	67
PEBA	SWNT	5	2.3	21	102	63.0	68
Matrimid	CNT-GO	5	4×10^{-5}	25	38.07	81.0	69
Pebax	MWCNT-COOH-4	4	3	30	24	81.0	70
Polyimide	MWCNT-COOH-OH	3	1	15	9.06	37.7	71
Pebax	MWNT	5	7	34.85	202	50.0	72
Pebax	MWNT	10	7	34.85	310	44.0	72
Pebax	MWNT	15	7	34.85	680	41.0	72
PSF	CNT/ZIF-301(6)	10	2	25	16	38.0	73
PSF	CNT/ZIF-301(12)	8	2	25	17	37.0	73
PSF	CNT/ZIF-301(18)	6	2	25	18	44.0	73
PSF	CNT/ZIF-301(24)	4	2	25	17	48.0	73
PSF	CNT/ZIF-301(30)	2	2	25	16	34.0	73
TFN	CNT-GO	1 : 1	4	70	66.3	47.1	74
BTDA-TDI/MDI (P84)	MWCNT	2	1	25	190.5	1.9	75
6FDA-TP polyimide	AP-SWNT	2	16.4	35	81	22	76

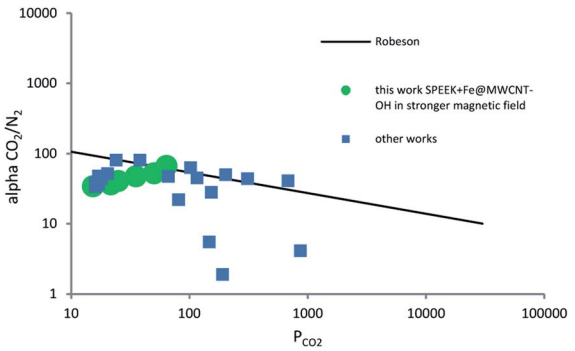

Fig. 10 Comparison of the dependence of the selectivity coefficient α_{CO_2/N_2} on the permeation coefficient P_{CO_2} for experimental and literature data.

It was found that the proposed hybrid membranes showed in many cases a marked improvement in selectivity and/or permeability compared to other membranes. Or their transport properties are comparable to the membranes representing the latest trends in CO_2 separation. It is especially visible in the case of the membrane with the greatest addition of Fe@MWCNT-OH (Fig. 10), which clearly crosses the Robeson line. A significant improvement in their transport properties may result from the synergistic effect of Fe@MWCNT-OH and SPEEK. Therefore, the proposed combination of a polymer matrix and an inorganic additive will allow the creation of a hybrid membrane material with potential application in improved CO_2 separation.

Conclusions

As part of the above article, novel inorganic–organic hybrid membranes were successfully synthesized, using SPEEK as a polymer matrix and Fe@MWCNT-OH as a filler. It was found that the introduction of nanofillers with an increased iron content (5.80 wt%) into the polymer matrix significantly improved gas transport (D, P, S and α_{CO_2/N_2}), magnetic, thermal, and mechanical parameters of the analyzed membranes, especially after the use of magnetic casting and chemical modification of the inorganic and organic phases. The use of the magnetic field in the production of membranes allowed for the proper arrangement and improvement of CNT dispersion in the polymer matrix and had a positive effect on their gas transport properties. The application of materials with paramagnetic and slightly ferromagnetic properties for the production of hybrid membranes made it possible to obtain a positive response to the magnetic field used. While the chemical modification of the polymer matrix and inorganic filler improved the interfacial compatibility and significantly improved the CO_2 separation efficiency, increasing both the selectivity coefficient α_{CO_2/N_2} values to 58.63 and the permeation coefficient P_{CO_2} to 59.56 barrer. The positive influence of the proposed modifications of both the polymer matrix and the inorganic additive on the CO_2 transport properties was found. Namely, the presence of polar sulfonic and sulfonate groups may promote CO_2–sulfone interactions, allowing a favorable affinity for CO_2. While better compatibility of the phases may mitigate the defects at their boundary and regulate the adequate fractional free volume to increase the CO_2 transport. On the other hand, the introduction of modified CNTs, which create "supra-structures" in the polymer matrix, may increase the rigidity of the polymer chains, extend the CO_2-philic pathways and increase the interaction with CO_2 electric quadrupole moment. The mechanical parameters (E and R_m) of the tested membranes were improved by increasing the addition of Fe@MWCNT-OH nanofiller (an increase in R_m from 33.09 to 68.64 MPa and E from 1.17 to 2.08 GPa). It was also found that the thermo-oxidative stability of the

tested composites increased with the increase of CNT content. The model developed by Chehrazi *et al.* turned out to be suitable for the description of CO_2 transport through the analyzed hybrid membranes (% AARE error was 12–16%). The proposed hybrid membranes seem to be suitable for the separation of CO_2 from gas mixtures, especially after the introduction of chemical modifications and the external magnetic field (increase in interfacial compatibility and affinity for CO_2). This type of solution, in the form of selective membranes Fe@MWCNT-OH/SPEEK for CO_2 separation, *e.g.*, from coal combustion flue gases, may be used in the power industry in the future. The comparison of the transport and separation properties of the tested membranes with the literature data shows that in most cases they are better or at least comparable. This may indicate the synergy effect between CNT and SPEEK and indicate their potential application in the future and the direction of further research.

Author contributions

Conceptualization, A. R. (Aleksandra Rybak), A. R. (Aurelia Rybak), S. B. (Sławomir Boncel) and S. K. (Spas D. Kolev); methodology, A. R. (Aleksandra Rybak), A. R. (Aurelia Rybak), W. K. (Waldemar Kaszuwara), S. B. (Sławomir Boncel), A. K. (Anna Kolanowska); software, A. R. (Aleksandra Rybak) and A. R. (Aurelia Rybak); writing – original draft preparation, A. R. (Aleksandra Rybak), A. R. (Aurelia Rybak), W. K. (Waldemar Kaszuwara), S. B. (Sławomir Boncel), A. K. (Anna Kolanowska) and S. K. (Spas D. Kolev). All authors have read and agreed to the published version of the manuscript.

Conflicts of interest

There are no conflicts to declare.

Acknowledgements

This publication was financed in frames of the statutory research BK 06/010/BK_22/0054.

Notes and references

1 A. Sattari, A. Ramazani, H. Aghahosseini and M. K. Aroua, The application of polymer containing materials in CO_2 capturing via absorption and adsorption methods, *J. CO2 Util.*, 2021, **48**, 101526, DOI: 10.1016/j.jcou.2021.101526.

2 Y. Han and W. S. W. Ho, Polymeric membranes for CO_2 separation and capture, *J. Membr. Sci.*, 2021, **628**, 119–244, DOI: 10.1016/j.memsci.2021.119244.

3 A. Kokkoli, Y. Zhan and I. Angelidaki, Microbial electrochemical separation of CO_2 for biogas upgrading, *Bioresour. Technol.*, 2018, **247**, 380–386, DOI: 10.1016/j.biortech.2017.09.097.

4 K. Huang, J.-Y. Zhang, F. Liu and S. Dai, Synthesis of porous polymeric catalysts for the conversion of carbon dioxide, *ACS Catal.*, 2018, **8**(10), 9079–9102, DOI: 10.1021/acscatal.8b02151.

5 N. Bryan, E. Lasseuguette, M. van Dalen, N. Permogorov, A. Amieiro, S. Brandani and M.-C. Ferrari, Development of mixed matrix membranes containing zeolites for post-combustion carbon capture, *Energy Procedia*, 2014, **63**, 160–166, DOI: 10.1016/j.egypro.2014.11.016.

6 F. Wu, P. A. Dellenback and M. Fan, Highly efficient and stable calcium looping based pre-combustion CO_2 capture for high-purity H_2 production, *Mater. Today Energy*, 2019, **13**, 233–238, DOI: 10.1016/j.mtener.2019.05.013.

7 E. I. Koytsoumpa, C. Bergins and E. Kakaras, The CO_2 economy: review of CO_2 capture and reuse technologies, *J. Supercrit. Fluids*, 2018, **132**, 3–16.

8 C. H. Yu, C. H. Huang and C. S. Tan, A Review of CO_2 Capture by Absorption and Adsorption, *Aerosol Air Qual. Res.*, 2012, **12**, 745–769, DOI: 10.4209/aaqr.2012.05.013.

9 B. Li, Y. Duan, D. Luebke and B. Morreale, Advances in CO_2 capture technology: a patent review, *Appl. Energy*, 2013, **102**, 1439–1447.

10 M. Kumar, M. Hemant, K. Balsora and P. Varshney, Progress and trends in CO_2 capture/separation technologies: a review, *Energy*, 2012, **46**, 431–441.

11 A. E. Creamer and B. Gao, Carbon-Based Adsorbents for Postcombustion CO_2 Capture: A Critical Review, *Environ. Sci. Technol.*, 2016, **50**, 7276–7289.

12 I. Ghiata and T. Al-Ansariab, A review of carbon capture and utilisation as a CO_2 abatement opportunity within the EWF nexus, *J. CO2 Util.*, 2021, **45**, 101432.

13 S. Sun, H. Sun, P. T. Williams and C. Wu, Recent advances in integrated CO_2 capture and utilization: a review, *Sustainable Energy Fuels*, 2021, **5**, 4546–4559.

14 P. Madejski, K. Chmiel, N. Subramanian and T. Kus, Methods and Techniques for CO_2 Capture: Review of Potential Solutions and Applications in Modern Energy Technologies, *Energies*, 2022, **15**, 887, DOI: 10.3390/en15030887.

15 N. Shreyash, M. Sonker, S. Bajpai, S. K. Tiwary, M. A. Khan, S. Raj, T. Sharma and S. Biswas, The Review of Carbon Capture-Storage Technologies and Developing Fuel Cells for Enhancing Utilization, *Energies*, 2021, **14**, 4978, DOI: 10.3390/en14164978.

16 A. I. Osman, M. Hefny, M. I. A. Abdel Maksoud, *et al.*, Recent advances in carbon capture storage and utilisation technologies: a review, *Environ. Chem. Lett.*, 2021, **19**, 797–849, DOI: 10.1007/s10311-020-01133-3.

17 A. Adamu, F. Russo-Abegão and K. Boodhoo, Process intensification technologies for CO_2 capture and conversion – a review, *BMC Chem. Eng.*, 2020, **2**, 2, DOI: 10.1186/s42480-019-0026-4.

18 M. Ahmadi, S. Janakiram, Z. Dai, L. Ansaloni and L. Deng, Performance of Mixed Matrix Membranes Containing Porous Two-Dimensional (2D) and Three-Dimensional (3D) Fillers for CO_2 Separation, *Membranes*, 2018, **8**, 50, DOI: 10.3390/membranes.8030050.

19 T. D. Kusworo, B. Budiyono, A. F. Ismail and A. Mustafa, Fabrication and Characterization of Polyimide-CNTs hybrid membrane to enhance high performance CO_2

separation, *Int. J. Sci. Eng.*, 2015, **8**(2), 115–119, DOI: 10.12777/ijse.8.2.115-119.

20 E. V. Perez, K. J. Balkus, J. P. Ferraris and I. H. Musselman, Mixed-matrix membranes containing MOF-5 for gas separations, *J. Membr. Sci.*, 2009, **328**, 165–173, DOI: 10.1016/j.memsci.2008.12.006.

21 J. Ahmad and M.-B. Hagg, Development of matrimid/zeolite 4A mixed matrix membranes using low boiling point solvent, *Sep. Purif. Technol.*, 2013, **115**, 190–197, DOI: 10.1016/j.seppur.2013.04.049.

22 S. Sridhar, B. Smith, M. Ramakrishna and T. M. Aminabhavi, Modified poly (phenylene oxide) membranes for the separation of carbon dioxide from methane, *J. Membr. Sci.*, 2006, **280**, 202–209, DOI: 10.1016/j.memsci.2006.01.019.

23 V. A. Bershtein, L. M. Egorova, P. N. Yakushev, G. Georgoussis, A. Kyritsis, P. Pissis, P. Sysel and L. Brozova, Molecular dynamics in nanostructured polyimide-silica hybrid materials and their thermal stability, *J. Polym. Sci., Part B: Polym. Phys.*, 2002, **40**, 1056, DOI: 10.1002/polb.10162.

24 T. S. Chung, L. Y. Jiang, Y. Li and S. Kulprathipanja, Mixed matrix membranes comprising organic polymers with dispersed inorganic fillers for gas separation, *Prog. Polym. Sci.*, 2007, **32**, 483, DOI: 10.1016/j.progpolymsci.2007.01.008.

25 D. Luebke, C. Myers and H. Pennline, Hybrid Membranes for Selective Carbon Dioxide Separation from Fuel Gas, *Energy Fuels*, 2006, **20**, 1906–1913, DOI: 10.1021/ef060060b.

26 D. Q. Vu, W. J. Koros and S. J. Miller, Mixed matrix membranes using carbon molecular sieves: I. preparation and experimental results, *J. Membr. Sci.*, 2003, **211**, 311–334, DOI: 10.1016/S0376-7388(02)00429-5.

27 R. M. Dukali, I. Radovic, D. B. Stojanovic, P. S. Uskokovic, N. Romcevic and V. Radojevic, Preparation, characterization and mechanical properties of $Bi_{12}SiO_{20}$-PMMA composite films, *J. Alloys Compd.*, 2014, **583**, 376–381, DOI: 10.1016/j.jallcom.2013.08.206.

28 H. Vinh-Thang and S. Kaliaguine, Predictive Models for Mixed-Matrix Membrane Performance: A Review, *Chem. Rev.*, 2013, **113**, 4980–5028, DOI: 10.1021/cr3003888.

29 Z. He, I. Pinnau and A. Morisato, Nanostructured poly(4-methyl-2-pentyne)/silica hybrid membranes for gas separation, *Desalination*, 2002, **146**, 11–15, DOI: 10.1016/S0011-9164(02)00463-0.

30 P. Sysel, E. Minko, M. Hauf, K. Friess, V. Hynek, O. Vopicka and K. Pilnacek, Mixed matrix membranes based on hyperbranched polyimide and mesoporous silica for gas separation, *Desalin. Water Treat.*, 2011, **34**, 211–215, DOI: 10.5004/dwt.2011.2859.

31 T. Suzuki and Y. Yamada, Physical and gas transport properties of novel hyperbranched polyimide/silica hybrid membranes, *Polym. Bull.*, 2005, **53**, 139–146, DOI: 10.1007/s00289-004-0322-9.

32 V. Krystl, J. Hradil, B. Bernauer and M. Kocirik, Heterogeneous membranes based on zeolites for separation of small molecules, *React. Funct. Polym.*, 2001, **48**, 129–139, DOI: 10.1016/S1381-5148(01)00047-5.

33 J. . Huang, X. Li, L. Luo, H. Wang, X. Wang and K. Li, Releasing silica-confined macromolecular crystallization to enhance mechanical properties of polyimide/silica hybrid fibers, *Compos. Sci. Technol.*, 2014, **101**, 24–31, DOI: 10.1016/j.compscitech.2014.06.022.

34 M. Ionita, E. Vasile, L. E. Crica, S. I. Voicu, A. M. Pandele, S. Dinescu, L. Predoiu, B. Galateanu, A. Hermenean and M. Costache, Synthesis, characterization and in vitro studies of polysulfone/graphene oxide composite membranes, *Composites, Part B*, 2015, **72**, 108–115, DOI: 10.1016/j.compositesb.2014.11.040.

35 K. G. Chandrappa and T. V. Venkatesha, Generation of Co_3O_4 microparticles by solution combustion method and its Zn–Co_3O_4 composite thin films for corrosion protection, *J. Alloys Compd.*, 2012, **542**, 68–77, DOI: 10.1016/j.jallcom.2012.07.067.

36 R. M. Khafagy, Synthesis, characterization, magnetic and electrical properties of the novel conductive and magnetic PANI/$MgFe_2O_4$ nanocomposite having the core–shell structure, *J. Alloys Compd.*, 2011, **509**, 9849–9857, DOI: 10.1016/j.jallcom.2011.07.008.

37 S. Boncel, A. P. Herman and K. Z. Walczak, Magnetic carbon nanostructures in medicine, *J. Mater. Chem.*, 2012, **22**, 31–37, DOI: 10.1039/C1JM13734D.

38 J. Bok-Badura, A. Jakobik-Kolon, M. Turek, S. Boncel and K. Karon, A versatile method for direct determination of iron content in multi-wall carbon nanotubes by inductively coupled plasma atomic emission spectrometry with slurry sample introduction, *RSC Adv.*, 2015, **5**, 101634–101640, DOI: 10.1039/C5RA22269A.

39 C. Oueiny, S. Berlioz and F. X. Perrin, Carbon nanotube–PANI composites, *Prog. Polym. Sci.*, 2014, **39**, 707–748, DOI: 10.1016/j.progpolymsci.2013.08.009.

40 A. Muhulet, F. Miculescu, S. I. Voicu, F. Schütt, V. K. Thakur and Y. K. Mishra, Fundamentals and scopes of doped carbon nanotubes towards energy and biosensing applications, *Mater. Today Energy*, 2018, **9**, 154–186, DOI: 10.1016/j.mtener.2018.05.002.

41 B. Wu, X. Li, D. An, S. Zhao and Y. Wang, Electro-casting aligned MWCNTs/polystyrene composite membranes for enhanced gas separation performance, *J. Membr. Sci.*, 2014, **462**, 62–68, DOI: 10.1016/j.memsci.2014.03.015.

42 D. Sieffert and C. Staudt, Preparation of hybrid materials containing copolyimides covalently linked with carbon nanotubes, *Sep. Purif. Technol.*, 2011, **77**, 99–103, DOI: 10.1016/j.seppur.2010.11.026.

43 A. R. Kim, M. Vinothkannan, M. H. Song, J. Y. Lee, H. K. Lee and D. J. Yoo, Amine functionalized carbon nanotube (ACNT) filled in sulfonated poly (ether ether ketone) membrane: Effects of ACNT in improving polymer electrolyte fuel cell performance under reduced relative humidity, *Composites, Part B*, 2020, **188**, 107890, DOI: 10.1016/j.compositesb.2020.107890.

44 A. L. Khan, X. Li and I. F. J. Vankelecom, Mixed-gas CO_2/CH_4 and CO_2/N_2 separation with sulfonated PEEK membranes, *J. Membr. Sci.*, 2011, **372**, 87–96, DOI: 10.1016/j.memsci.2011.01.056.

45 N. Zhang, D. Peng, H. Wu, Y. Ren, L. Yang, X. Wu, Y. Wu, Z. Qu, Z. Jianga and X. Cao, Significantly enhanced CO_2 capture properties by synergy of zinc ion and sulfonate in Pebax-pitch hybrid membranes, *J. Membr. Sci.*, 2018, **549**, 670–679, DOI: 10.1016/j.memsci.2017.10.054.

46 H. Wu, X. Shen, T. Xua, W. Hou and Z. Jiang, Sulfonated poly (ether ether ketone)/amino-acid functionalized titania hybrid proton conductive membranes, *J. Power Sources*, 2012, **213**, 83–92, DOI: 10.1016/j.jpowsour.2012.04.003.

47 S. Boncel, A. P. Herman, S. Budniok, R. G. Jędrysiak and A. Jakobik-Kolon, In vitro targeting and selective killing of T47D breast cancer cells by purpurin and 5-fluorouracil anchored to magnetic CNTs: nitrene-based functionalization versus uptake, cytotoxicity, and intracellular fate, *ACS Biomater. Sci. Eng.*, 2016, **2**(8), 1273–1285, DOI: 10.1021/acsbiomaterials.6b00197.

48 A. Zniszczoł, A. P. Herman, K. Szymanska, J. Mrowiec-Białon, K. Z. Walczak, A. Jarzebski and S. Boncel, Covalently immobilized lipase on aminoalkyl-, carboxy- and hydroxy-multi-wall carbon nanotubes in the enantioselective synthesis of Solketal esters, *Enzyme Microb. Technol.*, 2016, **87–88**, 61–69, DOI: 10.1016/j.enzmictec.2016.02.015.

49 A. Rybak, A. Rybak, W. Kaszuwara, S. Awietjan, R. Molak, P. Sysel and Z. J. Grzywna, The magnetic inorganic-organic hybrid membranes based on polyimide matrices for gas separation, *Composites, Part B*, 2017, **110**, 161–170, DOI: 10.1016/j.compositesb.2016.11.010.

50 A. Rybak, A. Rybak and P. Sysel, Modeling of Gas Permeation through Mixed-Matrix Membranes Using Novel Computer Application MOT, *Appl. Sci.*, 2018, **8**(7), 1166–1185, DOI: 10.3390/app8071166.

51 A. Rybak, A. Rybak, W. Kaszuwara and M. Nyc, Metal substituted sulfonated poly (2,6-dimethyl-1,4-phenylene oxide) hybrid membranes with magnetic fillers for gas separation, *Sep. Purif. Technol.*, 2019, **210**, 479–490, DOI: 10.1016/j.seppur.2018.08.032.

52 A. Rybak, Z. J. Grzywna and P. Sysel, Mixed matrix membranes composed of various polymer matrices and magnetic powder for air separation, *Sep. Purif. Technol.*, 2013, **118**, 424–431, DOI: 10.1016/j.seppur.2018.08.032.

53 A. Rybak and W. Kaszuwara, Magnetic properties of the magnetic hybrid membranes based on various polymer matrices and inorganic fillers, *J. Alloys Compd.*, 2015, **648**, 205–214, DOI: 10.1016/j.jallcom.2015.06.197.

54 A. Rybak, A. Rybak, W. Kaszuwara, S. Awietjan and J. Jaroszewicz, The rheological and mechanical properties of magnetic hybrid membranes for gas mixtures separation, *Mater. Lett.*, 2016, **183**, 170–174, DOI: 10.1016/j.matlet.2016.07.078.

55 A. Rybak, A. Rybak, W. Kaszuwara, S. Awietjan, P. Sysel and Z. J. Grzywna, The studies on novel magnetic polyimide inorganic–organic hybrid membranes for air separation, *Mater. Lett.*, 2017, **208**, 14–18, DOI: 10.1016/j.matlet.2017.04.147.

56 R. Hamilton and O. Crosser, Thermal Conductivity of Heterogeneous two-component systems, *Ind. Eng. Chem. Fundam.*, 1962, **1**, 187–191, DOI: 10.1021/i160003a005.

57 D. Y. Kang, C. W. Jones and S. Nair, Modeling molecular transport in composite membranes with tubular fillers, *J. Membr. Sci.*, 2011, **381**, 50–63, DOI: 10.1016/j.memsci.2011.07.015.

58 E. Chehrazi, A. Sharif, M. Omidkhah and M. Karimi, Modeling the Effects of Interfacial Characteristics on Gas Permeation Behavior of Nanotube–Mixed Matrix Membranes, *ACS Appl. Mater. Interfaces*, 2017, **9**, 37321–37331, DOI: 10.1021/acsami.7b11545.

59 D. Witkowska, *Basics of Econometrics and Forecasting*, Economic Publishing House, Krakow, 2006.

60 S. M. S. Al-Mufti, M. M. Ali and S. J. A. Rizvi, Synthesis and structural properties of sulfonated poly ether ether ketone (SPEEK) and Poly ether ether ketone (PEEK), *AIP Conf. Proc.*, 2020, **2220**, 020009, DOI: 10.1063/5.0001760.

61 S. Boncel, S. W. Pattinson, V. Geiser and M. S. P. Shaffer, En route to controlled catalytic CVD synthesis of densely packed and vertically aligned nitrogen-doped carbon nanotube arrays, *Beilstein J. Nanotechnol.*, 2014, **5**, 219–233, DOI: 10.3762/bjnano.5.24.

62 H. Kumazawa, J.-S. Wang, T. Fukuda and E. Sada, Permeation of carbon dioxide in glassy poly (ether imide) and poly (ether ether ketone) membranes, *J. Membr. Sci.*, 1994, **93**, 53–59, DOI: 10.1016/0376-7388(94)85015-1.

63 A. Ahmad, Z. Jawad, S. Low and S. Zein, A cellulose acetate/multi-walled carbon nanotube mixed matrix membrane for CO_2/N_2 separation, *J. Membr. Sci.*, 2014, **451**, 55–66.

64 H. Cong, J. Zhang, M. Radosz and Y. Shen, Carbon nanotube composite membranes of brominated poly(2,6-diphenyl-1,4-phenylene oxide) for gas separation, *J. Membr. Sci.*, 2007, **294**, 178–185.

65 H.-H. Tseng, I. A. Kumar, T.-H. Weng, C.-Y. Lu and M.-Y. Wey, Preparation and characterization of carbon molecular sieve membranes for gas separation—the effect of incorporated multi-wall carbon nanotubes, *Desalination*, 2009, **240**(1–3), 40–45.

66 R. Borgohain, N. Jain, B. Prasad, B. Mandal and B. Su, Carboxymethyl chitosan/carbon nanotubes mixed matrix membranes for CO_2 separation, *React. Funct. Polym.*, 2019, **143**, 104331.

67 A. R. Moghadassi, Z. Rajabi, S. M. Hosseini and M. Mohammadi, Preparation and Characterization of Polycarbonate-Blend-Raw/Functionalized Multi-Walled Carbon Nano Tubes Mixed Matrix Membrane for CO_2 Separation, *Sep. Sci. Technol.*, 2013, **48**, 1261–1271.

68 B. Yu, H. Cong, Z. Li, J. Tang and X. S. Zhao, Pebax-1657 nanocomposite membranes incorporated with nanoparticles/colloids/carbon nanotubes for CO_2/N_2 and CO_2/H_2 separation, *J. Appl. Polym. Sci.*, 2013, **130**, 2867–2876.

69 X. Li, L. Ma, H. Zhang, S. Wang, Z. Jiang, R. Guo, H. Wu, X. Cao, J. Yang and B. Wang, Synergistic effect of combining carbon nanotubes and graphene oxide in mixed matrix membranes for efficient CO_2 separation, *J. Membr. Sci.*, 2015, **479**, 1–10.

70 S. A. Habibiannejad, A. Aroujalian and A. Raisi, Pebax-1657 mixed matrix membrane containing surface modified

multi-walled carbon nanotubes for gas separation, *RSC Adv.*, 2016, **6**, 79563–79577.

71 H. Sun, T. Wang, Y. Xu, W. Gao, P. Li and Q. J. Niu, Fabrication of polyimide and functionalized multi-walled carbon nanotubes mixed matrix membranes by in situ polymerization for CO_2 separation, *Sep. Purif. Technol.*, 2017, **177**, 327–336.

72 D. Zhao, J. Ren, Y. Wang, Y. Qiu, H. Li, K. Hua, X. Li, J. Ji and M. Deng, High CO_2 separation performance of Pebax®/CNTs/GTA mixed matrix membranes, *J. Membr. Sci.*, 2017, **521**, 104–113.

73 M. Sarfraz and M. Ba-Shammakh, Harmonious interaction of incorporating CNTs and zeolitic imidazole frameworks into polysulfone to prepare high performance MMMs for CO_2 separation from humidified post combustion gases, *Braz. J. Chem. Eng.*, 2018, **35**, 217–228.

74 K. C. Wong, P. S. Goh, T. Taniguchi, A. F. Ismail and K. Zahri, The role of geometrically different carbon-based fillers on the formation and gas separation performance of nanocomposite membranes, *Carbon*, 2019, **149**, 33–44.

75 N. Sazali, W. N. W. Salleh, A. F. Ismail, K. C. Wong and Y. Iwamoto, Exploiting pyrolysis protocols on BTDA-TDI/MDI (P84) polyimide/nanocrystalline cellulose carbon membrane for gas separations, *J. Appl. Polym. Sci.*, 2018, **136**, 136.

76 Q. Zhang, S. Li, C. Wang, H.-C. Chang and R. Guo, Carbon nanotube-based mixed-matrix membranes with supramolecularly engineered interface for enhanced gas separation performance, *J. Membr. Sci.*, 2020, **598**, 117794.